"Polar mutagenesis of bacterial transcriptional units using Cas12a"

Antoine Graffeuil[1], Bernt Eric Uhlin[1] and David A. Cisneros[1]*

[1]Department of Molecular Biology, Umeå University, Umeå, Sweden.

*Corresponding author david.cisneros@umu.se

Abstract

Bacterial genes are often organized in functionally related transcriptional units or operons. One such example is the *fimAICDFGH* operon, which codes for type I fimbriae in *Escherichia coli*. We tested the hypothesis that markerless polar mutations could be efficiently engineered using CRISPR/Cas12a in the *fim* operon. Cas12a-mediated engineering of a terminator sequence inside the *fimA* gene occurred with efficiencies between 10 and 30%, whilst other types of mutations, such as a 97 bp deletion, occurred with 100% efficiency. Our results showed that some of the obtained mutants, including a single base substitution at the *fim* locus, had decreased mRNA levels of *fimA*, suggesting that the regulation of the *fim* operon was disrupted. On top, we corroborated the polar effect of these mutants by phenotypic assays and quantitative PCR, showing up to a 43 fold decrease in expression of genes downstream *fimA*. We believe this strategy could be useful in engineering the transcriptional shut-down of multiple genes in one single step.

Short title: Polar mutagenesis with Cas12a

24 **Introduction**

25

26 The evolutionary success of operons has been attributed to their contribution to the organization of
27 metabolic pathways, which ultimately allowed organisms to become less dependent on exogenous
28 sources of organic compounds (1). Importantly this relationship was maintained during evolution
29 for many metabolic pathways and was probably enhanced by horizontal gene transfer (1). Genes
30 within operons are co-transcribed from a single promoter but it has been shown that the mRNA of
31 each open reading frame (ORF) has a distinct folding from their neighbouring genes and this
32 feature directly influences its translation efficiency (2). Other features regulating operon expression
33 and function in *cis* include attenuators, terminators and processive aniterminators (reviewed in
34 (3,4)). All these elements of regulation depend on the formation of RNA secondary structures. We
35 asked ourselves if sequences with such a tendency to generate secondary structures could be
36 easily engineered in the *E. coli* chromosome using CRISPR/Cas technologies. CRISPR/Cas
37 genome editing in *E. coli* (5), opened the possibility of marker-less genetic engineering with single
38 base resolution. Therefore, it is possible to now generate multi-scale libraries of mutants in a few
39 days (6). We chose to engineer a completely synthetic terminator sequence (7) in the *fim* operon of
40 *E. coli*.

41

42 *Escherichia coli* is a research and synthetic biology work-horse. Thanks to the extent of the
43 knowledge available on its metabolism, it provides a playground in which bottom-up and top-down
44 approaches have the potential to intertwine. The possibility of easily controlling whole
45 transcriptional units would serve multiple purposes. For example one aspect poorly appreciated in
46 synthetic biology is metabolic burden (8). Protein synthesis has been calculated to be the most
47 expensive step (ATP-wise) involved in cell growth, compared to the biosynthesis of its building
48 blocks which uses only a small fraction of ATP (9). Therefore shutting down the synthesis of
49 unnecessary operons during specific growth conditions could contribute significantly to balance the

50 burden while expressing heterologous operons. Another example is shutting down or the re-
51 direction of competing metabolic routes (10). In this known issue, the bioinformatic analysis of
52 competing or converging metabolic routes will be essential (11). Alternative approaches to shut
53 down multiple genes, such as CRISPR/Cas9 multiplex gene repression or large fragment deletions
54 are available and have different advantages (12,13) to our approach. Therefore, the strategy
55 presented in this study opens another possibility to investigate, with one step, the effect of
56 competing transcriptional units arranged in operons on metabolic burden and compound
57 biosynthesis. Finally, virulence factors and antibiotic resistance genes in bacteria tend to cluster in
58 so called pathogenicity islands, and their removal or shutting down using CRISPR/Cas
59 technologies is a potential strategy to use as antibiotics (14).
60

61 Type one fimbriae are adhesive surface appendages present mainly in Enterobacteriaceae that
62 were first shown to agglutinate red-blood cells (15). They are composed of a main pilin subunit
63 repeated in the order of hundreds to thousands and are assembled at the surface by an outer
64 membrane usher. At the tip of the filament the so called minor pilins are assembled in a specific
65 order. The most distal pilin to the cell (FimH) functions as an adhesin (16,17). In the case of *E. coli*
66 type I fimbriae the FimH adhesin is inhibited by D-mannose residues and α-methyl-mannoside and
67 they recognize mannosylated receptors (16–18). Its role in virulence in uropathogenic strains of *E.*
68 *coli* has been established for a long time (19,20). However, it's role in mammalian persistent
69 intestinal colonization has only been recently studied. Indeed, it has been shown that the FimH
70 adhesin is essential for intestinal colonization of uropathogenic *E. coli* (21). How each fimbrial
71 system present in symbiotic *E. coli* (22) strains contributes to intestinal colonization of symbiotic
72 strains has not been yet studied *in vivo*.
73

74 The *fim* operon is a good system to test an engineered polar effect, for various reasons: Firstly, the
75 architecture of the *fim* operon is such that the gene coding for the major and most abundant

76 component of the pilus is the first to be transcribed followed by the assembly machinery. This gives
77 the advantage that disruption of this gene inactivates its functionality and any polar effect would
78 disrupt the function of the subunits important for assembly. Secondly, although the regulation of its
79 transcription is complex, it is chiefly determined by an invertible element upstream of the promoter
80 (fimAp), which acts as an ON/OFF switch.
81

82 The regulation of the mannose-dependent adhesion type I fimbriae is complex but has been
83 studied *in vitro* for decades. It has been shown to be regulated by various genes including NanR
84 and NagC (trough sialic acid and GlcNAc) (23), Lrp, (24,25), H-NS (26) and IHF (27). All these
85 elements mainly regulate the frequency of inversion of the invertible switch. The molecule
86 (p)ppGpp also regulates the *fim* switch (28).
87

88 In this study we introduce a terminator sequence with a strong secondary structure to disrupt the
89 transcription of the *fim* operon. We showed that this sequence is easy to introduce by
90 CRISPR/Cas12a engineering and that the engineered strains have a predictable phenotypic
91 outcome.
92

93

Results

Design of *fimA-targeting* crRNA and donor oligos

We wanted to disrupt the *fim* operon using Cas12a by introducing a range of different markerless mutations in the *fimA* gene including the insertion of a terminator sequence (Fig. 1). We designed a crRNA targeting the *E. coli fimA* gene. To introduce polar and nonpolar mutations in the *fim* operon we designed two complementary oligos for each mutation to form dsDNA donor molecules for homologous recombination. The recombination of these oligos disrupts the binding site of the Cas12a-crRNA complex and permits the positive selection of mutant cells (29).

To introduce a premature stop codon in the *fimA* gene, we designed dsDNA donor oligos in which a single bp change disrupted the PAM sequence for crRNA1 and introduced a stop codon (TAA) after 106 bp ($fimA_{A106T}$) of the start codon. To introduce a deletion in the *fimA (ΔfimA)* gene, we designed dsDNA donor oligos containing homology recombination sequences upstream and downstream of the crRNA recognition site to delete 97 bp introducing a stop codon after 75 bp of the start codon.

To engineer a polar mutagenesis strategy, we designed two different donor oligos to introduce a terminator sequence in the *fimA* gene. The first oligo contained the sequences for homologous recombination exactly as the deletion donor oligos but with the L3S2P56 terminator sequence in between at nucleotide position 75 ($fimA_{75}$*::L3S2P56*, called here Term1). The second donor oligos were similar but the upstream homologous region corresponded to the leader of the *fimA* gene. Therefore, these oligos introduce a terminator sequence at the start codon ($fimA_{1}$*::L3S2P56*, called here Term2).

119 **Mutagenesis of the *fimA gene***

120

121 Terminator sequences have a strong tendency to form secondary structures and therefore we
122 asked ourselves if such sequences could be readily used as DNA donors for CRISPR/Cas12a
123 mutagenesis. To test this hypothesis we simply electroporated *E. coli* cells carrying the plasmid
124 pKD46-Cas12a (29) with the annealed dsDNA donor oligos and a plasmid encoding crRNA1. We
125 analysed transformants by colony PCR using oligos that amplify a segment of the *fimA* gene
126 surrounding the site of crRNA targeting. For the stop codon mutant ($fimA_{A106T}$) using crRNA1, we
127 picked five colonies and performed colony PCR. The size of the PCR fragment did not appear to
128 change as compared to wild type (WT) *E. coli* (Fig 2). We purified these PCR products and
129 submitted them for Sanger sequencing. Four of the products showed the specific T->A substitution
130 that introduces a premature stop codon. For the deletion mutant, the PCR fragment showed a
131 noticeable change in migration compared to WT (Fig 2). Ten out of ten colonies picked showed the
132 deletion (S1 Fig.). For the insertion of a terminator sequence only three out of ten and one out of
133 ten colony PCRs showed a change in migration for the Term1 and Term2 mutations, respectively
134 (Fig. 1 and S1 Fig). All together these results show that the engineering of terminator sequences is
135 possible but with lower efficiencies compared to the engineering of single base substitutions and
136 deletions which had high efficiencies.

137

138 **Phenotypic analysis of *fimA* mutants**

139

140 To characterise the effect of the different mutations, we verified the functionality of the *fim* operon
141 by a phenotypic assay. We performed agglutination assays of *Saccharomyces cerevisiae* cells (Fig
142 3A-C). Overnight cultures of WT and *fimA* mutants *E. coli* strains were mixed with a drop of a yeast
143 suspension over a glass plate. Mixing WT *E. coli* leads *to* agglutination of the yeast cells, which
144 appeared as white, macroscopically visible aggregates (Fig 3D). Contrastingly, mixing *Shigella*

145 *flexneri* M90T, which is known not to express fimbrial genes (30), produced no yeast aggregates
146 (Fig 3E). Mixing each of our *fimA* mutants with the yeast suspension produced no agglutination
147 (Fig 3F-I). There was no difference between the stop codon mutant ($fimA_{A106T}$), deletion and
148 terminator mutants (Ter1 and Ter2), which suggests that the disruption of even one base
149 introducing a stop codon was enough to disrupt the functionality of the *fim* operon.
150

151 **Plasmid trans-complementation of the *fimA* mutants**
152

153 To verify the efficiency of the different mutations in exerting a polar effect, we verified the
154 functionality of the *fim* operon by a phenotypic assay. We repeated the agglutination assays in WT
155 and mutant strains carrying a plasmid expressing *fimA* (Fig 4). Each strain was transformed by the
156 trans-complementing plasmid and an empty vector as negative control. WT *E. coli* carrying the
157 empty vector agglutinated *S. cerevisiae* as expected and the expression of plasmid encoded *fimA*
158 did not change the appearance of the agglutination reaction (Fig 4A-B), suggesting that neither of
159 the plasmids cause an effect on agglutination. Trans-complementation of both the stop codon
160 ($fimA_{A106T}$) and deletion *fimA* mutants resulted in yeast agglutination (Fig 4C-D and Fig 4E-F),
161 suggesting that the mutations did not introduce any effect on genes downstream of *fimA*, which
162 code for the assembly machinery, and that expression of a functional copy of this gene rendered
163 these strains agglutination-positive. In contrast, the strains carrying the empty vector were
164 agglutination-negative. Trans-complementation of both Term1 and Term2 mutants with the empty
165 vector or the plasmid expressing *fimA,* resulted in no yeast agglutination (Fig 4G-H and Fig 4I-J).
166 This suggests that the functionality of the *fim* operon was completely disrupted downstream of
167 *fimA* in these two mutants and suggested that the transcription of genes downstream *fimA::*
168 *L3S2P56* terminators was disrupted.
169

170 **Measurement of mRNA levels of *fimA* and *fimI***

171

172 We wanted to quantify the extent of a polar effect in all the mutants obtained. We used qPCR to
173 measure the levels of *fimA* and *fimI*. We designed two sets of primers that allowed for the
174 estimation of the levels of these two genes (Fig 1B). We performed qPCR using as template cDNA
175 derived from mRNA obtained from *E. coli* cultures grown in the same conditions as those used for
176 the phenotypic assays. First, we estimated the amount of the *fimI* mRNA relative to *fimA.* This
177 represents an unbiased measurement that does not depend on the ON/OFF state of the fimAp.
178 Relative expression of *fimI* in WT *E. coli* was ~2.5 times lower to *fimA* (Table 1). The median
179 relative expression of *fimI* in the stop and deletion mutants was lower but in the same order of
180 magnitude (Fig 5A). The median relative expression of *fimI* in the Term1 and Term2 mutants was
181 considerably lower (Fig 5A). The relative expression fold change for the Term1 and Term2 mutants
182 was 9 and 43 fold, respectively (Table 1). These results suggest that at least an estimated 9 fold
183 change in expression is necessary to disrupt the functionality of the *fim* operon downstream of
184 *fimA*.

185 We wanted to measure the levels of *fimI* and *fimA* mRNA levels with respect to housekeeping
186 genes. We designed sets of primers for the housekeeping genes *hcaT* and *cysG*, which have been
187 shown to have stable expression (31). We obtained the average Δct with respect to these two
188 genes and normalized it to the WT control performed the day of the experiment. The levels of *fimA*
189 varied in all the mutants as well as the levels of *fimI* (Fig 5B). However for three out of four mutants
190 the expression of *fimA* and *fimI* was lower.

191

192 We were puzzled by the small but measurable changes of mRNA levels in the stop and deletion
193 mutants (Fig. 5B). To further investigate this phenomenon we decided to create two different stop
194 codon mutants. We co-introduced in *E. coli* plasmids encoding crRNA2 and crRNA3 (Fig 1) with
195 donor template oligos introducing a stop codon instead of the PAM sequence containing the
196 plasmid pKD46-Cas12a. For crRNA2 the donor oligos introduced the mutations T103A, T104A

197 (*fimA*$_{T103A,T104A}$) to disrupt the PAM sequence. For crRNA3 the donor oligo introduced the mutations
198 A158T,A159T, A160T,C161A, C162A (*fimA*$_{A158T,A159T,A160T,C161A,C162A}$). Two clones of each of these
199 mutants were selected and analysed by qPCR measurements of *fimI* and *fimA.* The median
200 relative expression of *fimI* to *fimA in* these two new mutants was also lower but in the same order
201 of magnitude of mutants carrying the allele *fimA*$_{A106T}$ (Fig 5A, orange and yellow circles). This result
202 suggests that the reduced levels of *fimA* expression are consistent in all three stop codon mutants.
203

204 **Observation of a *fimA* terminator mutant by AFM**

205

206 We wanted to observe the formation of fimbriae by Atomic Force Microscopy (AFM) and
207 agglutination in previously described favourable conditions. Fluorescence microscopy
208 measurements have shown an increase of fimbriae in static cultures of *E. coli* strain MG1655 (32).
209 We grew WT *E. coli* in and the Ter2 mutant expressing *fimA* from a plasmid on static cultures to
210 observe if there was any formation of fimbriae. To prepare the AFM samples in a way that it
211 introduced the least amount of manipulations, we diluted the static culture in deionized water to an
212 OD600 of 0.05 and we immobilized a drop of this suspension on freshly cleaved mica for 20
213 minutes. After the incubation period the mica was gently washed with more deionized water. In the
214 wild type strain expressing plasmid-encoded *fimA*, we observed bacteria showing the classical type
215 I fimbriae (Fig. 6A and 6A inset). However in the Ter2 mutant expressing plasmid-encoded *fimA* we
216 did not observe any formation of fimbriae (Fig. 6A). In some cells, only the formation of flagella
217 could be observed and (Fig.6A inset). To confirm the absence of functional fimbriae in this mutant,
218 we repeated the yeast agglutination assay after static growth conditions (Fig. 6B). As a negative
219 control we incubated this time the wild type strain with α-methyl-mannoside. The wild type strain
220 expressing plasmid-encoded *fimA* was agglutination-positive as shown in Fig. 4. However using
221 the same strain pre-incubated with α-methyl-mannoside completely abolished agglutination. This
222 confirms that agglutination is mediated by the mannose-dependent type I fimbriae encoded in the

223 *fim* operon. Agglutination by the Ter2 mutant expressing plasmid-encoded *fimA* did not
224 complement agglutination after having grown in static conditions and the agglutination reaction
225 appeared as the α-methyl-mannoside negative control. All these results confirm that the Ter2
226 mutant appears to have a *fim* negative phenotype even when *fimA* is expressed in *trans*.
227

228 **Table 1. Relative levels of *fimI* to *fimA* mRNA.**

Strain	Median Δct (*fimI* - *fimA*)*	Median Δct (*fimA* - *fimI*)	~Fold change inhibition
WT	0.39	2.6	1
Stop codon	0.10	9.8	4
ΔfimA	0.17	5.8	2
Term1	0.04	23.3	9
Term2	0.009	111.4	43

229 Table1. Relative levels of *fimI* transcript with respect to *fimA*. The median Δct values are
230 shown as in *Fig 5A. The fold change was calculated by dividing the median Δct (*fimI* –
231 *fimA*) of each mutant by the median value in the wild type.

232

233 **Discussion**

234

235 CRISPR/Cas technologies have become part of routine work in many laboratories. For the
236 synthetic biology field it opened the possibility of quickly engineer chromosomal loci. For
237 biotechnological purposes, it also opens the possibility to decrease the use of plasmids to produce
238 heterologous enzymes. Plasmids can be lost and impose extra metabolic burdens and regulatory
239 burdens that have to be taken into account when fine-tuning bio-production (reviewed in (8)). One
240 proposed approach is to iteratively test the effect of engineered mutations in strains to optimize this
241 process (33). However the effect of a mutation in a system often carries unpredictable or poorly
242 controlled consequences. In *E. coli*, 63% of its genes are organized in operons (34) and 40% are
243 organised in uber operons (35). In both of these organisation levels, genes tend to be related by
244 functional conservation across bacterial genomes (35). The possibility to transcriptionally shut-
245 down with one step a whole operon could contribute to the quick design and testing of strains with
246 more predictable outcomes if regulons and uber operons are taken into account.

247

248 In this study we used an artificial terminator sequence to shut down the transcription of the *fim*
249 operon. This designed artificial sequence has an extended secondary structure that has been
250 shown to improve transcriptional termination (7). We did not know whether such secondary
251 structures could impede the recombination process in the context of the donor homology
252 recombination oligonucleotides used for CRISPR/Cas genome engineering. The predictable
253 outcome from inserting this sequence in the *fim* operon is the premature transcriptional termination
254 of the genes coding for the type I fimbriae assembly machinery. Our results showed that indeed a
255 reduction of up to 43 fold in the expression of the *fim* machinery as measured by the expression of
256 *fimI.*

257

258 The efficiency of genome engineering strains has been shown to depend on the efficiencies of
259 gRNAs to direct Cas9 DNA cleavage and donor oligos (6). Using the same crRNA and target
260 sequence we saw efficiencies ranging from 10% to 100%. However the donor oligonucleotides
261 varied in homology arms and secondary structure. Therefore our results suggest that, as
262 suspected, these two parameters are important for bacterial genome engineering. Despite these
263 differences we could readily find mutants with inserted terminator sequences. Among the 582
264 terminator sequences characterised by Chen *et al.*, we decided to use an artificial terminator
265 sequence (L3S2P56) that showed to have low recombination rates (7), which would ensure more
266 stability within the *E. coli* chromosome. However we did not know whether this would decrease the
267 recombination mediated by homology arms upstream and downstream of the terminator sequence.
268 Our results show that this sequence was easily engineered using the Cas12a-encoding plasmids
269 designed by Yan *et al.* (29). These plasmids are easy to use and allow multiple rounds of
270 mutagenesis similar to previously reported Cas9 approaches (6). Cas12a also brings the
271 advantage that it processes its own crRNAs, which we think will allow certain flexibility in the future
272 when dealing with organisms with poorly characterised promoter sequences. All together this study
273 shows that it is possible to shut down the expression of a whole operon using an artificial
274 terminator. This approach could be complementary to other approaches that allow the
275 transcriptional repression of multiple genes such as the use of multiple gRNAs for transcriptional
276 repression (12) or the deletion of large genomic stretches (13). The use of Cas12a also facilitated
277 genome engineering, because its PAM sequence NTTT (AAAN in the bottom strand) can be easily
278 mutated to introduce a stop codon. Indeed here we showed a single base substitution ($fimA_{A106T}$)
279 disrupted PAM recognition and allowed the selection of *fimA* mutant strains.
280

281 The *fim* operon was an ideal study case because the phenotype is macroscopically observable and
282 the characterisation of the *fimA* mutants by yeast agglutination yielded predictable results.
283 Moreover, the extent of fimbriation is directly correlated to the state of the switch inside fimAp (32),
284 therefore for every *fimA* transcript observed the presence of a *fimI* transcript reflects the polarity of

285 the mutants generated here. Indeed, insertion of a terminator sequence abolished the trans-
286 complementation by a plasmid-encoded *fimA* gene. Less predictable phenotypes were obtained by
287 measuring the relative expression of *fimI* to *fimA* in typical laboratory conditions. Three out the four
288 mutants that were generated in this study, both polar and nonpolar, had reduced median levels of
289 *fimA transcript* and of the ratio *fimI/fimA* transcripts. This includes a single base substitution that
290 introduces a stop codon *(fimA$_{A106T}$).* Several possible explanations exist to accommodate this fact.
291 For example, it is known that ribosome binding protects mRNAs from RNase E degradation (36).
292 Therefore, one possible explanation would be that the premature stop codon introduced in
293 *fimA$_{A106T}$* and in the deletion mutant induces the premature release of ribosome (37,38) and at the
294 same time exposes the *fimA* transcript to degradation. Another more complicated involves the
295 stalling of ribosomes during translation, which may induce mRNA cleavage next to or at a stop
296 codon (39). An initial cleavage event could lead to further degradation by classical mRNA decay
297 pathways. However this could only make sense if the folding of the *fimA* mRNA would be
298 compromised and stalling would be induced by the mutations designed here. This can also be put
299 in the context of the recent discovery that the mRNA of individual genes within operons have a
300 unique secondary structure (2). Deletions smaller than a whole gene could affect the folding of an
301 individual genes' mRNA within an operon. Another possibility would be that there would be some
302 kind of positive feedback on type I fimbriae expression or functionality. On the conditions that we
303 assayed *fimA* expression, that is rich medium at 37 C, switching off dominates on fimAp (40).
304 Therefore, any kind of feedback would quickly result in *fimA* expression inhibition. Another
305 possibility would be that the mutation introduced in this study interferes with a differential stability
306 within *fim* genes' transcripts, which is an important element for other fimbrial systems (e.g, the *pap*
307 fimbrial operon from uropathogenic *E. coli*) (41). One final possibility is that expression of a
308 functional type I fimbriae system confers a growth advantage (32,42), although this has only been
309 proposed for static cultures. Alternatively, the peptide products of the stop codon mutants (~35
310 amino acids long and hydrophobic) could also be partially toxic and induce the selection of cells
311 with the *fim* switch in the off state. Although this would not apply to the terminator insertion at
312 position 1 (Ter2) mutant for which there should not be any partial *fimA* peptide product. Further

313 studies will be needed to clarify the role of the three stop codon mutants and deletion on the
314 expression of *fimA.* However, our results show that even a single nucleotide substitution can have
315 subtle but measurable changes at the transcriptional level within an operon when measured in
316 typical laboratory conditions.

317 The chromosome of *E. coli* encodes multiple fimbrial systems. However, in the conditions used in
318 this study, only the *fim* type I fimbriae are functional (22). The results shown in this study open the
319 possibility of quickly generating *E. coli* strains in which each fimbrial operon is inactivated. This
320 could be useful to see if any of these systems is essential under a particular growth condition.
321 Another future direction of interest is to characterise the effect of other *fimA* stop codon mutants on
322 the stability of its transcript. It would be crucial to determine if the effects observed here are gene
323 specific or can occur in many other premature stop codon mutants. This is important in the light
324 that introducing a premature stop codon is the easiest form to disrupt a gene using markerless
325 techniques such as Cas9- or Cas12a-mediated mutagenesis.
326

327 In summary, in this study we show that Cas12a can be used to introduce markerless insertions in
328 *E. coli* in one step and that this insertion can have strong secondary structures such as terminator
329 sequences without compromising too much the efficiency of the process. This approach allows the
330 transcriptional shut-down of whole operons as demonstrated for the case of the *fim* type I fimbriae
331 system. More importantly, this approach can be used to easily test the importance of whole
332 operons for the physiology of *E. coli* or its effect in the design of novel or artificial biosynthetic
333 pathways.

334

335 **Materials and Methods**

336

337 **Cas12a Mutagenesis.** To design Cas12a crRNA targeting *fimA* with no off-targets in *E. coli*
338 MG1655 (43), we used the webtool Chop-Chop (44) and crRNA ranking 1, 2 and 4 were selected
339 due to its closeness to the start codon. To introduce all the mutations designed in this study we
340 used the plasmids designed by Yan *et al.* (29) and followed their protocol with some modifications.
341 Cloning of crRNAs was done by annealing forward and reverse oligos at 95 °C and ramping the
342 temperature down at 2.55°C/minute. The oligos were then phosphorylated using polynucleotide
343 kinase (ThermoFisher). The plasmid pAC-crRNAred (29) was digested with BsaI-HF (New England
344 Biolabs), dephosphorylated with FastAP (ThermoFisher) and ligated to the annealed oligos. Donor
345 oligos were treated in the same way as crRNA oligos and their annealing was verified as
346 suggested by König *et al.* (45). The night before the experiment we grew from a glycerol stock *E.*
347 *coli* MG1655 carrying plasmid pKD46-Cas12a at 30 °C. The day of the experiment, 100 µl of
348 overnight culture was transferred to a new agar plate with 0.2% arabinose and four hours later
349 electrocompetent cells were prepared using the "rapid" protocol (46). These cells were co-
350 transformed by plasmids carrying one crRNA and an annealed pair of donor oligos. As a control
351 transformation we used a crRNA targeting the gene coding for GFP. Colony PCR was then
352 performed on transformants for genotyping. Each colony was resuspended in 20 µl water and
353 boiled for 5 minutes. One µl of this sample was used as template for PCR. Agarose gel
354 electrophoresis or Sanger sequencing was followed to determine the number of mutants. At least
355 two independent colonies of each mutant were selected for further analysis. After mutagenesis was
356 confirmed by sequencing, the strains were cured from the plasmids following the recommendations
357 of Yan *et al.* (29). We observed that this process had a 100% efficiency by growing the cells at 37
358 °C in 5% sucrose in very rich medium such as YT2X. Glycerol stocks were then prepared for each
359 clone. The structure of the L3S2P56 terminator was calculated with the Vienna websuite (47) and
360 visualised with Forna (48).

361

362 **Agglutination assay.** To observe yeast agglutination, wild type or mutant MG1655 was grown
363 overnight for 16 hours on Luria agar plates as described before (49). A 1 ul plastic loop was used
364 to take a colony from the plate and mixed with 200 µl of a *Saccharomyces cerevisiae* suspension
365 at OD 5 prepared from refrigerated baker's yeast. The loop was used to gently mix the two cell
366 populations and the appearance of white flocculent aggregates became clear for the wild type
367 strain in less than 30 seconds. *Shigella flexneri* 5A M90T *was* used as a negative control (50). To
368 perform this assay from static cultures, we repeated the same procedure but instead of using a
369 plastic loop we used 10 µl from strains grown overnight in 20 ml tryptic soy broth (TSB). The
370 agglutination took approximately 2-5 minutes in this case of the wild type strain expressing
371 plasmid-encoded *fimA*. As a negative control, 10 µl of a 3% (w/v) solution of α-methyl-mannoside
372 was added to a 10 µl suspension of wild type *E. coli* and pre incubated for 1 minute before
373 agglutination.
374

375 **RNA isolation.** To isolate RNA we used the modified method described by Blomberg *et al.* (51)
376 with one further modification. Namely, we grew cells in the same conditions assayed for
377 agglutination assays (overnight on Luria agar plates) on a lawn. The equivalent to half a plate was
378 scraped and dissolved immediately in DEPC treated water with 10% SDS, 20 mM sodium acetate
379 pH 4.8 and 10 mM EDTA and flash frozen in liquid nitrogen. Frozen cells were thawed and lysed
380 by incubating the samples for 5 min at 65 ºC. Total RNA was extracted by the hot-phenol method
381 (51). Residual DNA was digested by DNase I (ThermoFisher; 1 U/µg RNA, 60 min, 37 ºC) in the
382 presence of RNase inhibitor (Ribolock, ThermoFisher Scientific; 0.1 U/µl) followed by a clean-up
383 step of RNA by phenol/chloroform/isoamyl alcohol and precipitation with ethanol, 0.1 M sodium
384 acetate pH 5.5 and 20 µg of glycogen (ThermoFisher). Removal of residual DNA was verified by
385 PCR using *fimA* oligos. Complementary DNAs (cDNAs) were prepared from each RNA sample
386 using the RevertAid kit (ThermoFisher) according to the manufacturer instructions. As a control of
387 DNA contamination we prepare for each sample a sample without reverse transcriptase. (-RT
388 sample).

389

390 **qPCR analysis.** To perform qPCR we used SYBR Green master mix (ThermoFisher) according to
391 the manufacturer instructions. To analyse the expression of *fimA*, *fimI*, *hcaT* and *cysG*, we
392 designed specific oligos using primer BLAST (Table 2). We used an iCycler iQ5 (Bio-Rad) and for
393 each gene cDNAs generated from bacteria grown on plates and as a control we produced a
394 sample without reverse transcriptase (-RT) using the exact same RNA. We verified that for each
395 qPCR experiment we did not find any detectable signal in the -RT sample. Denaturation curves
396 were also used to verify the presence of a single product. We performed these controls for every
397 single biological replicate. To verify the linearity of each primer we diluted the cDNA obtained from
398 wild type *E. coli*, which always contained the highest amounts of *fimA and fimI* and verified that 10
399 times dilutions steps had a slope close to -3.3. We performed this calibration for many of our
400 experiments but not for all. Once we learned that the oligos showed a linear behaviour we trusted
401 our primers. To analyse qPCR data we used the iQ5 optical system software (Bio-Rad) obtained
402 the Δct from the suggested values of the software. We verified in any case manually that changes
403 in the threshold did not affect or bias the results. Each measurement was quantified using the
404 following formula: Δct=2^(ct1-ct2). Where ct is the threshold crossing value where the SYBR green
405 fluorescent signal appears. In the case of the *fimI* to *fimA* value reported in figure 5A we simply
406 report the Δct without any transformation. Despite the fact that ct values varied across
407 experiments, the *fimI* to *fimA* Δct was, in our hands, consistent across experiments within one
408 order of magnitude. To normalize the data of *fimA* and *fimI* against housekeeping genes we
409 obtained the Δct of each sample against the ct value of *cysG* and *hcaT* and the average of the two
410 values was obtained. The average Δct values of each sample was normalized against the Δct of
411 the wild type strain as a percentage. The ratio of the *fimI* to *fimA* expression was obtained by
412 dividing their normalized Δct values and expressed as a percentage.

413

414 **AFM.** To prepare AFM samples, punch-holed 1 cm pieces of muscovite mica were immobilized on

415 metal supports using double sided tape. The static cultures were diluted ten times on milliQ water.
416 A drop of 100 µl from the diluted bacterial suspension was afterwards placed on the mica right
417 after cleaving it with laboratory tape. The suspension was incubated for 20 minutes and the liquid
418 was exchanged three times with ultrapure milli Q water. The samples were placed in the chemical
419 hood and left to dry for a minimum of five minutes. The presence of bacteria on the mica was
420 verified using an optical system mounted on the AFM and a random area was selected for imaging.
421 The AFM imaging was performed in a MultiMode8 (Bruker) in force tapping mode using the
422 ScanAsyst software at a rate of 1 Hz using SCANAYST tips with a nominal spring constant of 0.4
423 N/m. Images shown in figure 6 show the error signal generated by the piezo (J scanner).

424 **Acknowledgements**

425

426 We thank the support of the Carl Tryggers Stiftelse för Vetenskaplig Forskning (projects CTS 15-96
427 and CTS18-65 awarded to David A. Cisneros), the Kempestiftelserna (projects JCK-1724 awarded
428 to Bernt Eric Uhlin and SMK 1860 awarded to David A. Cisneros). We also want to thank Ramon
429 Cervantes Rivera for helping with RNA purifications. We also thank Aster Assefa for her technical
430 assistance in qPCR and the creation of deletion mutants.

431

432

433 **References**

434 1. Fondi M, Emiliani G, Fani R. Origin and evolution of operons and metabolic pathways.
435 Research in Microbiology. 2009 Sep 1;160(7):502–12.
436 2. Burkhardt DH, Rouskin S, Zhang Y, Li G-W, Weissman JS, Gross CA. Operon mRNAs are
437 organized into ORF-centric structures that predict translation efficiency. Elife.
438 2017;6:e22037.
439 3. Merino E, Yanofsky C. Transcription attenuation: a highly conserved regulatory strategy
440 used by bacteria. Trends in Genetics. 2005 May 1;21(5):260–4.
441 4. Goodson JR, Winkler WC. Processive Antitermination. Microbiology Spectrum. 2018 Oct;
442 2020;6(5).
443 5. Jing W, Bikard D, Cox D, Zhang F, Marraffini LA. RNA-guided editing of bacterial genomes
444 using CRISPR-Cas systems. Nature biotechnology. 2013 Mar;31(3):233–239.
445 6. Zerbini F, Zanella I, Fraccascia D, König E, Irene C, Frattini LF, et al. Large scale validation
446 of an efficient CRISPR/Cas-based multi gene editing protocol in *Escherichia coli*. Microbial
447 cell factories. 2017;16(1):68.
448 7. Chen Y-J, Liu P, Nielsen AAK, Brophy JAN, Clancy K, Peterson T, et al. Characterization of
449 582 natural and synthetic terminators and quantification of their design constraints. Nature
450 Methods. 2013 Jun;10(7):659–664.
451 8. Wu G, Yan Q, Jones JA, Tang YJ, Fong SS, Koffas MAG. Metabolic Burden: Cornerstones
452 in Synthetic Biology and Metabolic Engineering Applications. Trends in Biotechnology.
453 2016 Aug 1;34(8):652–64.
454 9. Russell JB, Cook GM. Energetics of bacterial growth: balance of anabolic and catabolic
455 reactions. Microbiol Mol Biol Rev. 1995 Mar 1;59(1):48–62.
456 10. Solomon KV, Moon TS, Ma B, Sanders TM, Prather KLJ. Tuning Primary Metabolism for
457 Heterologous Pathway Productivity. ACS Synth Biol. 2013 Mar 15;2(3):126–35.
458 11. Kuwahara H, Alazmi M, Cui X, Gao X. MRE: a web tool to suggest foreign enzymes for the

459 biosynthesis pathway design with competing endogenous reactions in mind. Nucleic Acids
460 Res. 2016 Jul 8;44(W1):W217–25.
461 12. Cress BF, Toparlak ÖD, Guleria S, Lebovich M, Stieglitz JT, Englaender JA, et al.
462 CRISPathBrick: modular combinatorial assembly of type II-A CRISPR arrays for dCas9-
463 mediated multiplex transcriptional repression in *E. coli*. ACS synthetic biology.
464 2015;4(9):987–1000.
465 13. Su T, Liu F, Gu P, Jin H, Chang Y, Wang Q, et al. A CRISPR-Cas9 Assisted Non-
466 Homologous End-Joining Strategy for One-step Engineering of Bacterial Genome.
467 Scientific Reports. 2016 Nov 24;6(1):1–11.
468 14. Bikard D, Euler CW, Jiang W, Nussenzweig PM, Goldberg GW, Duportet X, et al. Exploiting
469 CRISPR-Cas nucleases to produce sequence-specific antimicrobials. Nat Biotechnol. 2014
470 Nov;32(11):1146–50.
471 15. Duguid JP, Smith IW, Dempster G, Edmunds PN. Non-flagellar filamentous appendages
472 ("fimbriae") and haemagglutinating activity in *Bacterium coli*. The Journal of pathology and
473 bacteriology. 1955;70(2):335–348.
474 16. Jones CH, Pinkner JS, Roth R, Heuser J, Nicholes AV, Abraham SN, et al. FimH adhesin
475 of type 1 pili is assembled into a fibrillar tip structure in the Enterobacteriaceae.
476 Proceedings of the National Academy of Sciences. 1995;92(6):2081–2085.
477 17. Krogfelt KA, Bergmans H, Klemm P. Direct evidence that the FimH protein is the mannose-
478 specific adhesin of *Escherichia coli* type 1 fimbriae. Infection and immunity.
479 1990;58(6):1995–1998.
480 18. Collier WA, De Miranda JC. [Bacterial hemagglutination. III. Mannose inhibition of *E. coli*
481 hemagglutination]. Antonie Van Leeuwenhoek. 1955;21(2):133–40.
482 19. Hultgren SJ, Porter TN, Schaeffer AJ, Duncan JL. Role of type 1 pili and effects of phase
483 variation on lower urinary tract infections produced by *Escherichia coli*. Infection and
484 immunity. 1985;50(2):370–377.
485 20. Wright KJ, Seed PC, Hultgren SJ. Development of intracellular bacterial communities of

486 uropathogenic *Escherichia coli* depends on type 1 pili. Cellular microbiology.
487 2007;9(9):2230–2241.
488 21. Spaulding CN, Klein RD, Ruer S, Kau AL, Schreiber HL, Cusumano ZT, et al. Selective
489 depletion of uropathogenic *E. coli* from the gut by a FimH antagonist. Nature. 2017
490 22;546(7659):528–32.
491 22. Korea C-G, Badouraly R, Prevost M-C, Ghigo J-M, Beloin C. *Escherichia coli* K-12
492 possesses multiple cryptic but functional chaperone–usher fimbriae with distinct surface
493 specificities. Environmental Microbiology. 2010;12(7):1957–77.
494 23. Sohanpal BK, El-Labany S, Lahooti M, Plumbridge JA, Blomfield IC. Integrated regulatory
495 responses of fimB to N-acetylneuraminic (sialic) acid and GlcNAc in *Escherichia coli* K-12.
496 PNAS. 2004 Nov 16;101(46):16322–7.
497 24. Gally DL, Rucker TJ, Blomfield IC. The leucine-responsive regulatory protein binds to the
498 fim switch to control phase variation of type 1 fimbrial expression in *Escherichia coli* K-12.
499 Journal of Bacteriology. 1994 Sep 1;176(18):5665–72.
500 25. Kroner GM, Wolfe MB, Freddolino PL. *Escherichia coli* Lrp regulates one-third of the
501 genome via direct, cooperative, and indirect routes. Journal of bacteriology.
502 2019;201(3):e00411–18.
503 26. O′gara JP, Dorman CJ. Effects of local transcription and H-NS on inversion of the fim
504 switch of *Escherichia coli*. Molecular Microbiology. 2000;36(2):457–66.
505 27. Eisenstein BI, Sweet DS, Vaughn V, Friedman DI. Integration host factor is required for the
506 DNA inversion that controls phase variation in *Escherichia coli*. PNAS. 1987 Sep
507 1;84(18):6506–10.
508 28. Aberg A, Shingler V, Balsalobre C. (p) ppGpp regulates type 1 fimbriation of *Escherichia*
509 *coli* by modulating the expression of the site-specific recombinase FimB. Molecular
510 microbiology. 2006;60(6):1520–1533.
511 29. Yan M-Y, Yan H-Q, Ren G-X, Zhao J-P, Guo X-P, Sun Y-C. CRISPR-Cas12a-Assisted
512 Recombineering in Bacteria. Appl Environ Microbiol. 2017 Sep 1;83(17).

513 30. Bravo V, Puhar A, Sansonetti P, Parsot C, Toro CS. Distinct mutations led to inactivation of
514 type 1 fimbriae expression in *Shigella spp.* PLoS ONE. 2015;10(3):e0121785.
515 31. Zhou K, Zhou L, Lim Q 'En, Zou R, Stephanopoulos G, Too H-P. Novel reference genes for
516 quantifying transcriptional responses of Escherichia coli to protein overexpression by
517 quantitative PCR. BMC Mol Biol. 2011 Apr 23;12:18.
518 32. Blomfield IC, McClain MS, Princ JA, Calie PJ, Eisenstein BI. Type 1 fimbriation and fimE
519 mutants of *Escherichia coli* K-12. Journal of Bacteriology. 1991 Sep 1;173(17):5298–307.
520 33. Van Dien S. From the first drop to the first truckload: commercialization of microbial
521 processes for renewable chemicals. Current Opinion in Biotechnology. 2013 Dec
522 1;24(6):1061–8.
523 34. Cao H, Ma Q, Chen X, Xu Y. DOOR: a prokaryotic operon database for genome analyses
524 and functional inference. Brief Bioinform. 2019 Jul 19;20(4):1568–77.
525 35. Che D, Li G, Mao F, Wu H, Xu Y. Detecting uber-operons in prokaryotic genomes. Nucleic
526 Acids Res. 2006 Apr 1;34(8):2418–27.
527 36. Richards J, Belasco JG. Obstacles to Scanning by RNase E Govern Bacterial mRNA
528 Lifetimes by Hindering Access to Distal Cleavage Sites. Molecular Cell. 2019 Apr
529 18;74(2):284-295.e5.
530 37. Laurberg M, Asahara H, Korostelev A, Zhu J, Trakhanov S, Noller HF. Structural basis for
531 translation termination on the 70S ribosome. Nature. 2008 Aug;454(7206):852–7.
532 38. Scolnick E, Tompkins R, Caskey T, Nirenberg M. Release factors differing in specificity for
533 terminator codons. Proc Natl Acad Sci U S A. 1968 Oct;61(2):768–74.
534 39. Hayes CS, Sauer RT. Cleavage of the A Site mRNA Codon during Ribosome Pausing
535 Provides a Mechanism for Translational Quality Control. Molecular Cell. 2003 Oct
536 1;12(4):903–11.
537 40. Gally DL, Bogan JA, Eisenstein BI, Blomfield IC. Environmental regulation of the fim switch
538 controlling type 1 fimbrial phase variation in *Escherichia coli* K-12: effects of temperature
539 and media. Journal of bacteriology. 1993;175(19):6186–6193.

540 41. Båga M, Göransson M, Normark S, Uhlin BE. Processed mRNA with differential stability in
541 the regulation of *E. coli* pilin gene expression. Cell. 1988 Jan 29;52(2):197–206.
542 42. Old DC, Duguid JP. Selective Outgrowth of Fimbriate Bacteria in Static Liquid Medium.
543 Journal of Bacteriology. 1970 Aug 1;103(2):447–56.
544 43. Guyer MS, Reed RR, Steitz JA, Low KB. Identification of a sex-factor-affinity site in *E. coli*
545 as γδ. In: Cold Spring Harbor symposia on quantitative biology. Cold Spring Harbor
546 Laboratory Press; 1981. p. 135–140.
547 44. Labun K, Montague TG, Gagnon JA, Thyme SB, Valen E. CHOPCHOP v2: a web tool for
548 the next generation of CRISPR genome engineering. Nucleic Acids Res. 2016 Jul
549 8;44(W1):W272–6.
550 45. König E, Zerbini F, Zanella I, Fraccascia D, Grandi G. Multiple Stepwise Gene Knockout
551 Using CRISPR/Cas9 in *Escherichia coli*. BIO-PROTOCOL. 2018;8(2).
552 46. Gonzales MF, Brooks T, Pukatzki SU, Provenzano D. Rapid Protocol for Preparation of
553 Electrocompetent *Escherichia coli* and *Vibrio cholerae*. JoVE (Journal of Visualized
554 Experiments). 2013 Oct 8;(80):e50684.
555 47. Gruber AR, Lorenz R, Bernhart SH, Neuböck R, Hofacker IL. The Vienna RNA Websuite.
556 Nucleic Acids Res. 2008 Jul 1;36(suppl_2):W70–4.
557 48. Kerpedjiev P, Hammer S, Hofacker IL. Forna (force-directed RNA): Simple and effective
558 online RNA secondary structure diagrams. Bioinformatics. 2015 Oct 15;31(20):3377–9.
559 49. Müller CM, Åberg A, Straseviçiene J, Em\Hody L, Uhlin BE, Balsalobre C. Type 1 fimbriae,
560 a colonization factor of uropathogenic *Escherichia coli*, are controlled by the metabolic
561 sensor CRP-cAMP. PLoS pathogens. 2009;5(2).
562 50. Sansonetti PJ, Kopecko DJ, Formal SB. Involvement of a plasmid in the invasive ability of
563 *Shigella flexneri*. Infection and immunity. 1982;35(3):852–860.
564 51. Blomberg P, Wagner EG, Nordström K. Control of replication of plasmid R1: the duplex
565 between the antisense RNA, CopA, and its target, CopT, is processed specifically in vivo
566 and in vitro by RNase III. The EMBO journal. 1990;9(7):2331–2340.

567 **Table 2 Strains used in this study.**
568

Name	Strain	Reference
Wild type	*Escherichia coli* MG1655	Guyer *et al.*
S. flexneri	*Shigella flexneri 5A M90T*	Sansonetti *et al.*
Stop1	*Escherichia coli* $fimA_{106T}$	This study
Stop2	*Escherichia coli* $fimA_{T103A,T104A}$	This study
Stop3	*Escherichia coli* $fimA_{A158T,A159T,A160T,C161A,C162A}$	This study
ΔfimA	*Escherichia coli* $fimA_{\Delta 76-172}$	This study
Term1	*Escherichia coli* $fimA_{75}$*::L3S2P56*	This study
Term2	*Escherichia coli* $fimA_{1}$*::L3S2P56*	This study

570 **Table 3**. Oligos used in this study.
571

Name	Sequence	Annotation
17-0001	GGCAATCGTTGTTCTGTCGG	FimA forward
17-0002	GAAGGTCGCATCCGCATTAG	FimA reverse
17-0003	GGCTCTGTCCCTCAGTTCTACAGCGGCTCTGGCCGCTGC CtaaGACAGGTTCGTACCGCATCGCTGGCACAGGAAGGA GCAAC	FimaA deletion donor oligo forward
17-0004	GTTGCTCCTTCCTGTGCCAGCGATGCGGTACGAACCTGT CttaGGCAGCGGCCAGAGCCGCTGTAGAACTGAGGGACA GAGCC	FimA deletion donor oligo reverse
17-0005	TGCCACGACGGTTAATGGTGGGACCGTTCACTTTTAAGG GGAAGTTGTTAACGCCGCTTGCGCAGTTGAT	fimA mutant 1 stop codon crRNA1
17-0006	ATCAACTGCGCAAGCGGCGTTAACAACTTCCCCTTAAAA GTGAACGGTCCCACCATTAACCGTCGTGGCA	fimA mutant 1 stop codon crRNA1
17-0007	CTGCCACGACGGTTAATGGTGGGACCGTTCACTAAAAAG GGGAAGTTGTTAACGCCGCTTGCGCAGTTGA	fimA mutant 2 stop codon crRNA2
17-0008	TCAACTGCGCAAGCGGCGTTAACAACTTCCCCTTTTTAG TGAACGGTCCCACCATTAACCGTCGTGGCAG	fimA mutant 2 stop codon crRNA2
17-0009	GCCGCTTGCGCAGTTGATGCAGGCTCTGTTGATCTTTAA GTTCAGTTAGGACAGGTTCGTACCGCATCGC	fimA mutant 3 stop codon crRNA3
17-0010	GCGATGCGGTACGAACCTGTCCTAACTGAACTTAAAGAT CAACAGAGCCTGCATCAACTGCGCAAGCGGC	fimA mutant 3 stop codon crRNA3
17-0013	TTAGAAATAGTTTTTTGAAAGGAAAGCAGCCTCGGTACC AAATTTTCGAAAAAAGACGCTGAAAAGCGTCTTTTTTCG TTTTGGTCCGACAGGTTCGTACCGCATCGCTGGCACAGG	fimA terminator2 at ATG forward
17-0014	CCTGTGCCAGCGATGCGGTACGAACCTGTCGGACCAAAA CGAAAAAAGACGCTTTTCAGCGTCTTTTTTCGAAAATTT GGTACCGAGGCTGCTTTCCTTTCAAAAAACTATTTCTAA	fimA terminator2 at ATG reverse
17-0015	CCTGTGCCAGCGATGCGGTACGAACCTGTCGGACCAAAA CGAAAAAAGACGCTTTTCAGCGTCTTTTTTCGAAAATTT GGTACCGAGGGCAGCGGCCAGAGCCGCTGTAGAACTGAG	fimA terminator2 inside forward
17-0016	CCTGTGCCAGCGATGCGGTACGAACCTGTCGGACCAAAA CGAAAAAAGACGCTTTTCAGCGTCTTTTTTCGAAAATTT GGTACCGAGGGCAGCGGCCAGAGCCGCTGTAGAACTGAG	fimA terminator2 inside reverse
17-0017	tagatAAGGGGAAGTTGTTAACGCCGCTT	fimA crRNA2 BsaI fw
17-0018	agacAAGCGGCGTTAACAACTTCCCCTTa	fimA crRNA2 BsaI rev
17-0019	tagatATCAACAGAGCCTGCATCAACTGC	fimA crRNA3 BsaI fw
17-0020	agacGCAGTTGATGCAGGCTCTGTTGATa	fimA crRNA3 BsaI rev
17-0021	tagatAAGTGAACGGTCCCACCATTAACC	fimA crRNA1BsaI fw
17-0022	agacGGTTAATGGTGGGACCGTTCACTTa	fimA crRNA1 BsaI rev
17-0042	CTGGAACCGTAACGCAGACT	FimA 2 Fw for terminator genotyping
17-0043	AGGCAACAGCGGCTTTAGAT	FimA 2 Rv for terminator genotyping
18-0012	ATCTTTTGGGGGAAAACTGTGC	qPCR fimA Fw 90 bp recognizes all mutants
18-0013	ATTTCTAAATCGACATGGGCAGT	qPCR fimA Rv 90 bp recognizes all mutants
17-0067	TGCTGCCAATGTTTGCTCTG	fimI qPCR Fwd 233pb
17-0068	TTCACTCACCACCGTGCTAC	fimI qPCR Rev
17-0073	tacgCCAAGCTTTGAAAGGAAAGCAGCATGAAAATTAAA AC	fimA-FW cloning pSU19 HindIII EcoRI
17-0074	gccagtGAATTCTTATTGATACTGAACCTTGAAGGTCG	fimA-rv cloning pSU19 HindIII EcoRI
17-0077	tagatCGTCGCCGTCCAGCTCGACCAGGA	crRNA BsaI GFP control fw
17-0078	agacTCCTGGTCGAGCTGGACGGCGACGa	crRNA BsaI GFP control rv

Figure 1

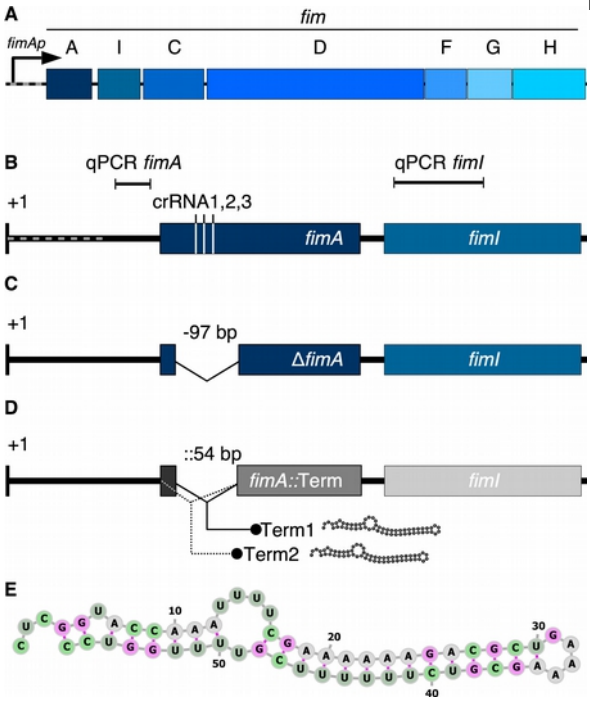

Fig 1. Design of Cas12a mutagenesis of the *fimAICDFGH* operon. A) The *Escherichia coli fim* operon is transcribed from a promoter (fimAp) containing an invertible element (grey dotted line) and *fimA* codes for the major fimbrial subunit, which was targeted by Cas12a. B) Enhanced view of the *fim* transcript from the +1 transcriptional start site. The regions amplified for qPCR analysis in the *fimA* and *fimI* genes are shown together with the homologous positions to the three crRNAs used in this study. A stop codon was introduced to substitute the PAM sequence to generate a stop codon mutant ($fimA_{A106T}$). C) Scheme of the 97 bp *fimA* deletion (*ΔfimA*) generated with a dsDNA donor oligo bearing 40 bp of homology. D) Scheme of the 54 bp *fimA* terminator insertion generated with a dsDNA donor oligo bearing a terminator sequence surrounded by 30 bp of homology. Two different insertions were generated: the first was generated at the site of the deletion shown in C ($fimA_{75}$*::L3S2P56*) and the second at the position of the start codon ($fimA_{1}$*::L3S2P56*) of the *fimA* gene. E) Secondary structure prediction of the L3S2P56 terminator used to create the mutants shown in D.

Figure 2

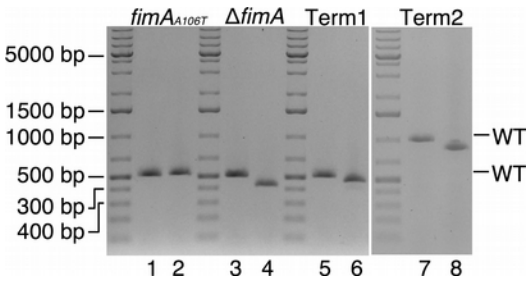

Fig. 2. Detection of *fimA* mutants by PCR. Lanes 1, 3, 5, show a 514 bp PCR product generated by primers that amplify a segment of the wild type *fimA* gene. Lane 2 shows the unchanged PCR product when amplifying the stop codon mutant generated with crRNA1 ($fimA_{A106T}$). Lanes 4 and 6 show the PCR product generated after amplifying DNA from the deletion mutant (*ΔfimA,* 420 bp) and the internal terminator insertion (Ter1, 474 bp), respectively. Lanes 7 show a 988 bp PCR product generated by primers that amplify a segment of wild type *fimA* including the leader sequence and lane 8 shows the 870 bp PCR product generated with DNA from the second terminator insertion (Ter2), which is at the start codon position.

Supplementary Figure 1

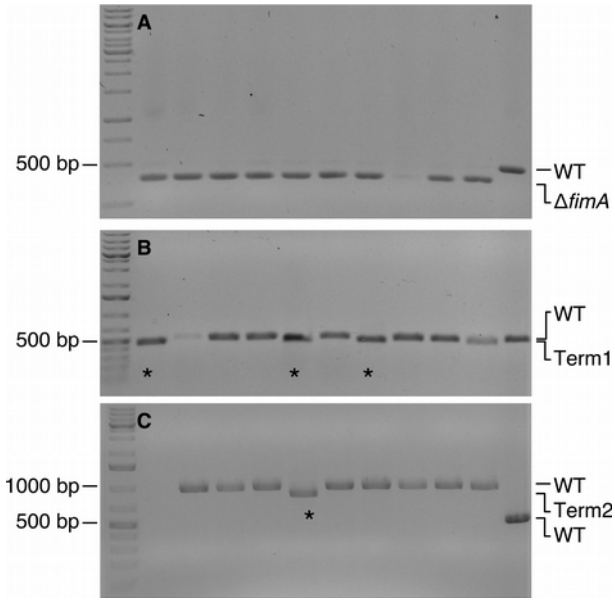

Supplementary Fig 1. Efficiency of *fimA* mutant generation with Cas12a. A) 10/10 *E. coli* colonies co-transformed with crRNA1 and the donor oligo carrying a 97 bp *fimA* deletion tested positive as detected by colony PCR. B) 3/10 *E. coli* colonies co-transformed with crRNA1 and the donor oligo carrying a 54 bp *fimA* terminator insertion tested positive as detected by colony PCR (marked with *). C) 1/10 *E. coli* colonies co-transformed with crRNA1 and the donor oligo carrying a 54 bp terminator insertion at the *fimA* start codon tested positive as detected by colony PCR (marked with *).

Figure 3

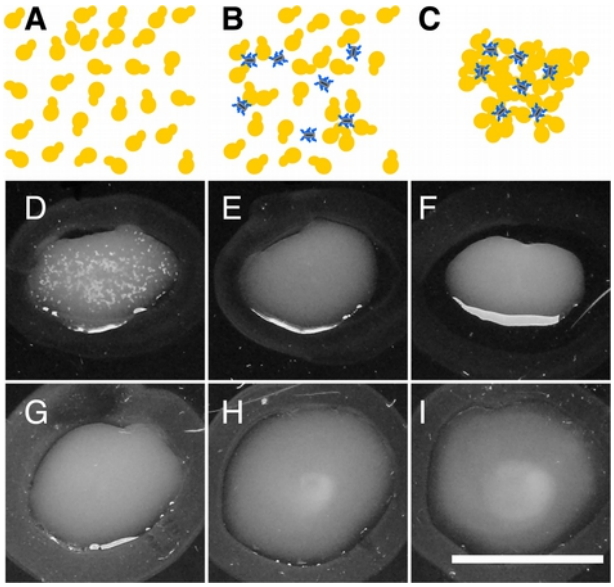

Fig 3. Agglutination assay of *fimA* mutants. A) A suspension of *Saccharomyces cerevisiae* is spread on glass plate. B) Using a loop the strain to be tested is mixed and the fimbriae subunit FimH recognizes mannose residues on the surface of the cells. C) The polyvalent binding of fimbriae to cells causes an agglutination chain reaction, which is macroscopically visible. D-I) Agglutination reaction for the following strains: D) WT *E. coli*, E) *Shigella flexneri* (negative control), F) Stop codon mutant ($fimA_{A106T}$) G) Δ*fimA* H) $fimA_{75}$*::L3S2P56* I) $fimA_{1}$*::L3S2P56.* Scale bar 2 cm.

Figure 4

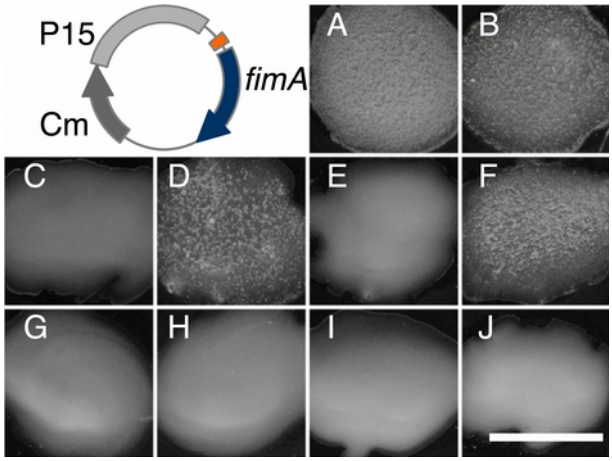

Fig 4. Plasmid complementation of *fimA* mutants. *fimA* was expressed from a plasmid with a P15 origin of replication and lac promoter (orange) without IPTG induction. The empty vector, pSU19, was used as negative control. A-J) Agglutination reaction for the following strains: A) WT *E. coli* + empty vector. B) WT *E. coli* + *fimA* plasmid. C) $fimA_{A106T}$ + empty vector. D) $fimA_{A106T}$ + *fimA* plasmid. E) Δ*fimA* + empty vector. F) Δ*fimA* + *fimA* plasmid. *G*) Term1 ($fimA_{75}$*::L3S2P56*) + empty vector. H) Term1($fimA_{75}$*::L3S2P56*) + *fimA* plasmid. I) Term2 ($fimA_{1}$*::L3S2P56*) + empty vector. J) Term2 ($fimA_{1}$*::L3S2P56*) + *fimA* plasmid. Scale bar 2 cm.

Figure 5

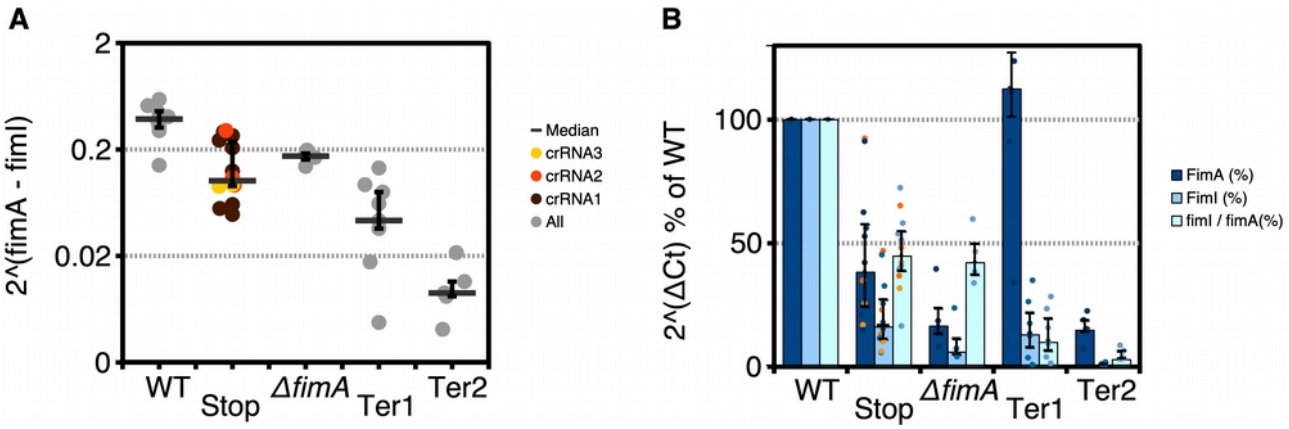

Fig 5. Quantitative PCR analysis. Two PCR product were used to quantify the expression of *fimA* and *fimI* (see scheme in Fig. 1). A) *fimI* expression normalized to *fimA* expression. Each data point represents a biological replicate and the median is shown (–). The error bars show the 25th and 75th percentile. B) Same data as in A) but shown as median ΔCt expression of *fimA* and *fimI* normalized to the housekeeping genes *hcaT* and *cysG* and expressed as percent of the wild type. Orange and yellow data points represent the stop codon mutants generated with crRNA1 and crRNA2 as in A. The median ratio of the normalized *fimI/fimA* expression is shown. The error bars show the 25th and 75th percentile. The labels represent the following mutants: Stop ($fimA_{A106T}$), deletion mutant Δ*fimA*), Ter1 ($fimA_{75}$*::L3S2P56*), Ter2 ($fimA_{1}$*::L3S2P56*).

Figure 6

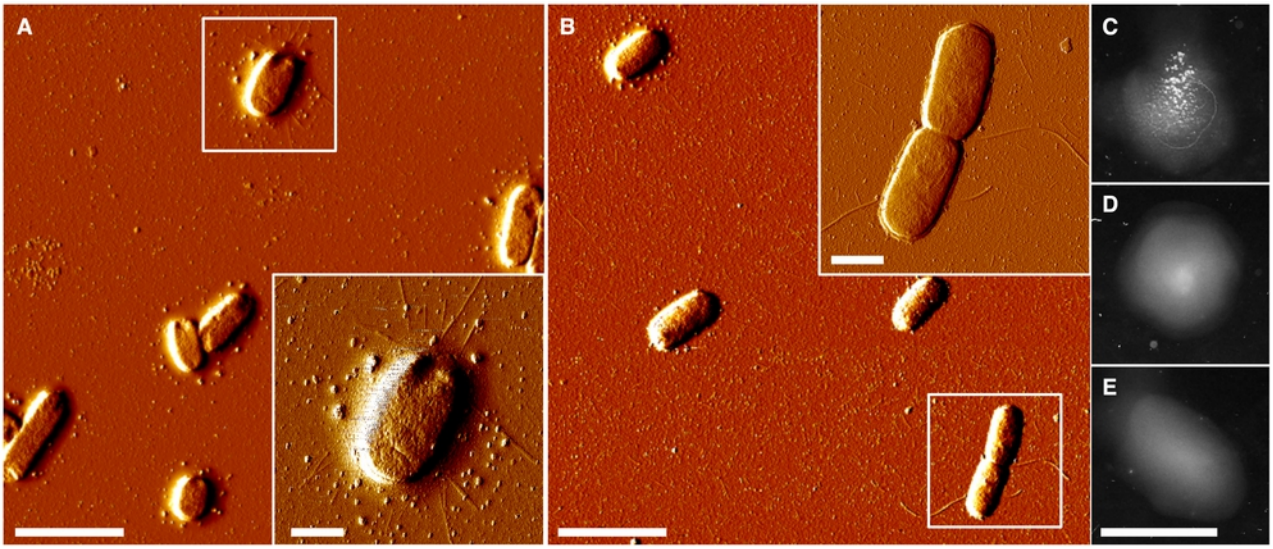

Figure 6. Atomic force microscopy (AFM) and agglutination of static cultures. A) AFM imaging of wild-type *E. coli* + *fimA* plasmid grown in static conditions. A cell showing fimbriae is shown in the inset. B) AFM imaging of Term2 mutant of *E. coli* (*fimA*$_1$*::L3S2P56*) + *fimA* plasmid grown in static conditions. A cell showing flagella is shown as an inset. C) Yeast agglutination assay of wild-type *E. coli* + *fimA* plasmid grown in static conditions. D) Yeast agglutination assay of of wild-type *E. coli* + *fimA* plasmid grown in static conditions in the presence of α-methyl-mannoside. E) Yeast agglutination assay of Term2 mutant of *E. coli* (*fimA*$_1$*::L3S2P56*) + *fimA* plasmid grown in static conditions. Scale bars: A-B) 4 µm. A-B) insets 1 µm. C-E) 2 cm.